European Journal of Wood and Wood Products (2021) 79:611–627
https://doi.org/10.1007/s00107-020-01636-4

ORIGINAL ARTICLE

Investigating the suitability of fly ash/metakaolin-based geopolymers reinforced with South African alien invasive wood and sugarcane bagasse residues for use in outdoor conditions

H. O. Olayiwola[1] · S. O. Amiandamhen[1] · M. Meincken[1] · L. Tyhoda[1]

Received: 4 May 2020 / Accepted: 17 November 2020 / Published online: 3 January 2021

Abstract
The prevailing approach of total clearing to contain the spread of invasive plants (IP) in South Africa is generating enormous lignocellulosic wastes. This study examined the possibility of utilizing these wastes in the production of geopolymer composites for use in outdoor environments. Untreated wood particles from *Acacia mearnsii* and *A. longifolia*, as well as sugarcane bagasse residues, were incorporated into a geopolymer matrix developed from a binary precursor system of 75% fly ash and 25% metakaolin. The variables considered included precursor-activator ratio (PA), curing pattern (CP), lignocellulosic material (LM), and alkali concentration (Mcon). The production process was established using a mixed factorial experimental design. PA and CP were considered at 2 levels, while LM and MCon were considered at 3 levels. The density of the boards exceeded 1 g cm^{-3} and are classified as high-density boards. The boards have comparable sorption properties to the cement-bonded particleboard according to the EN 632-2: 2007 standard. However, only *A. longifolia* boards produced with 12 M NaOH and PA ratio of 2:1 met the mechanical strength requirements. Thermogravimetric analysis revealed that the boards are thermally stable. These results have shown that South African woody IPs are suitable for geopolymer wood composites, but there is still concern about their durability in the alkaline matrix. Scanning electron microscopy micrographs indicated mineralization of the particles and a partial degradation of hemicellulose was confirmed by Fourier transform infrared spectroscopy. Although the degraded components did not prevent geopolymer setting, there is need to further investigate the extent and means of preventing degradation as this can derail the intended use of the product.

1 Introduction

South Africa (SA) has been reported to have the largest proportion of invasive plants (IPs) in the world (Le Maitre et al. 2000). The IPs affect the biological diversity of natural ecosystem, human livelihood, and economic development. These impacts have prompted the government to institute various programmes and policies aimed at eradicating IPs on both state and privately owned lands (Shackleton 2016). However, the prevailing control approach is based on total clearing which generates excessive lignocellulosic waste and negatively impacts the environment (Amiandamhen et al. 2018b). Similarly, the sugar industries in SA generate about 6 million tonnes of sugarcane (*Saccharum officinarum*) bagasse (SCB) annually, but only 6–7% is used for making animal feeds, paper and furfural products. SCB is the fibrous residue left after the juice has been extracted from the sugarcane stalk. The rationale for the selection of SCB in this study was based on the volume of residue generated and the associated disposal problems. Biomass residues, wastepaper, fly ash, and slag from the processing of ores constitute about 80 million tonnes of waste generated in South Africa annually. 74 million tonnes (or 93%) of this waste is disposed through landfilling (DEA 2012). Landfilling option is currently not economically sustainable due to the high cost of landfilling and is not environmentally friendly due to toxic air emissions and greenhouse gases. To discourage the use of landfills, the SA government embarked on several initiatives by increasing legislative and landfilling taxes. This measure has inadvertently created opportunities for more beneficial uses of waste streams.

One of several alternatives to add value to the cleared woody IPs and SCB lies in the manufacturing of wood composite products for low-cost building construction. Previous

✉ L. Tyhoda
ltyhoda@sun.ac.za

[1] Department of Forest and Wood Science, Stellenbosch University, Stellenbosch, South Africa

studies have incorporated wood particles from invasive species and agricultural crop residues into a phosphate matrix to produce phosphate-bonded composite products for use in building applications (Amiandamhen et al. 2016, 2018b). These composite products had promising properties, but recent studies have revealed that the high cost of this particular binder could prohibit its eventual use in the production of board products (Chimphango 2020). The use of alternative binders, such as ordinary Portland cement (OPC) and polymeric resins, widely used in construction and wood composite industries has been shown to increase greenhouse gases and formaldehyde emissions, which have the potential to negatively affect the environment and human lives. The production of cement accounts for 5.6% of the total 9.9 ± 0.5 GtC (gigatons of carbon) emission in 2016 (Le Quéré et al. 2018). In addition, volatile formaldehyde emitted from polymeric resins has been classified as Category-1 known human carcinogen by the International Agency for Research on Cancer (IARC) (Van Langenberg et al. 2010). The global awareness regarding these pressing challenges has stimulated renewed interest in finding alternative green binders that exhibit adequate properties and low environmental impact.

Geopolymers are emerging alternative inorganic binders with excellent potential to substitute the conventional binders in different applications from an environmental and a technical point of view (Mellado et al. 2014). Geopolymers not only provide performance comparable to OPC in many applications, they also allow for a huge reduction in global warming potential by about 60% (Habert et al. 2011) and energy consumption by about 70% compared to OPC (Castaldelli et al. 2016). They are produced by geo-synthesis of materials rich in aluminosilicate with an alkaline metal solution at ambient or slightly elevated temperature (Alomayri et al. 2013). Other advantages include early strength development of about 70% within 3–4 h of the curing period (Kong and Sanjayan 2008), high acid and fire resistance, excellent adherence to aggregates, and immobilization of toxic and hazardous materials (Alomayri et al. 2013; Chen 2014; Duan et al. 2016). These properties and the ability to synthesize them from industrial waste such as fly ash and slag make them promising alternative binders in wood-based composites. However, geopolymers are brittle and exhibit low tensile and flexural strengths like other inorganic cementitious binders.

Different synthetic materials such as high tenacity (HT) carbon fibres, E-glass, polyvinyl alcohol (PVA), polyvinyl chloride (PVC), polypropylene (PP), basalt and micro steel fibres (MSF) have been incorporated in geopolymers developed from different precursor materials to improve its strength properties. Yunsheng et al. (2008) reinforced fly ash-based geopolymer with short PVA fibres. An optimum volume fraction of 2.0% ameliorated the brittle properties of the product. The fibres changed the impact failure mode of the composite product from brittle to ductile, resulting in a great increase in impact toughness. Natali et al. (2011) embedded HT carbon, PVA, PVC and E-glass in metakaolin-based geopolymer. The addition of the fibres improved the structural strength by 30–70% compared to unreinforced geopolymer. Zhang et al. (2014) observed improved mechanical properties with the addition of carbon fibres in metakaolin-based geopolymer, while Korniejenko et al. (2015) also reported enhanced mechanical properties of fly ash-based geopolymer with the addition of PP fibres. The addition of PP to geopolymer matrix improves the flexural strength of these materials. Composites made with addition of 15% vol. of reinforcing fibres had the best flexural strength. These synthetic fibres influence high strength in the composites, but they are very expensive and their production is highly energy intensive. Being non-biodegradable, there is a serious concern about their disposal at the end of their life cycle (Herrmann et al. 1998; Pacheco-Torgal and Jalali 2011). This inarguably hinders the overall objective of developing a sustainable eco-friendly low-cost material. Consequently, natural fibres are being envisaged as possible alternatives in geopolymer composite production.

Lignocellulosic materials (LM) offer numerous advantages over synthetic materials in composite manufacturing. They are relatively low cost, widely available, sustainable, biodegradable and possess high strength to weight ratio (Mohr et al. 2004; Pacheco-Torgal and Jalali 2011). Encapsulation of LM in the geopolymer matrix is relatively new in the wood-based composites sector, and their use for structural applications has not been extensively studied. The first structural application of wood-geopolymer composite dates back to the period between 1973 and 1976 (Davidovits 2008). Fire-resistant chipboard panels were developed by sandwiching a wooden core between two layers of geopolymeric coatings. Recent investigations, however, have shown that LM can be incorporated into both unary and binary precursor based geopolymeric binder to produce composite products. Alomayri et al. (2014) studied the mechanical properties of a fly ash-based geopolymer reinforced with cotton fabric at elevated temperature. The precursor was activated using a combination of sodium silicate to sodium hydroxide at a ratio of 2.5, but the concentration of NaOH was not indicated. The resulting geopolymer boards were cured at 85 °C for 24 h. Chen et al. (2014) added sorghum fibres pre-treated with 2 M NaOH to reinforce fly ash-based geopolymers activated with 10 M NaOH and concluded that the addition of fibres decreased the workability and unit weight of geopolymer pastes. Fibre content up to 2% increased both the tensile and flexural strength of the geopolymer composites. Duan et al. (2016) encapsulated a mixture of unnamed wood particles in a geopolymer matrix made of Class F fly ash activated with sodium silicate and

10 M NaOH at a ratio of 8:1. The addition of sawdust up to 20% improved the mechanical properties of the composites. The targeted application areas for the composite products were not mentioned in these previous investigations. Binary systems of precursors utilizing a combination of fly ash and metakaolin or slags have been reported to have superior strength compared to geopolymers made with either precursor (Buchwald et al. 2007; Chareerat et al. 2006; Fernandez-Jimenez et al. 2008; Neupane et al. 2016; Puertas et al. 2000; Valencia Saavedra and Mejía de Gutiérrez 2017). Sarmin (2016), Sarmin and Welling (2016) and Sarmin and Welling (2015) added unnamed wood particles to a binary precursor made from fly ash and metakaolin to produce a lightweight material. The addition of wood particles improved the strength, but no mention was made about how the inherent wood properties influenced the performance of the geopolymer product. This study seeks to address these shortcomings and further explores the potentials of utilizing agricultural residues and invasive species in geopolymer product development, using a mixed factorial design.

The major drawback of natural fibre when compared to the synthetic fibres is the variation in their compositions (Li et al. 2006) and issues associated with their durability in alkaline matrices (Amiandamhen et al. 2019). The lignin and hemicellulose components of LM are prone to degradation in alkaline environments leading to weakening of the fibre structure. Although geopolymer is also highly alkaline in nature, it exhibits quite a different chemistry to cement hydration. The current study investigated the properties of fly ash/metakaolin-based geopolymers reinforced with wood particles from IP and SCB targeted for use in outdoor conditions such as wall cladding, roof and floor tiles. By reducing landfills, the innovation in this study will create opportunities for more effective and sustainable utilization of industrial waste in development of eco-friendly building materials.

2 Materials

2.1 Lignocellulosic materials and geopolymer precursors

The lignocellulosic materials (LM) used in the study are particles of acacia wood species and sugarcane bagasse (SCB) fibres. Acacia wood (*A. longifolia* and *A. mearnsii)* was supplied by Casidra, Paarl in the Western Cape, South Africa, while SCB was sourced from TSB Sugar Pty Ltd., South Africa. The wood was debarked, chipped, and milled in a hammer mill fitted with a 1 mm sieve. The milled samples (Fig. 1) were conditioned at 20 °C and 65% relative humidity for 96 h before use. A binary precursor system comprising of low calcium fly ash (FA) and metakaolin (MK) was utilized in this study. The FA, classified as Class S (SFA) according to the SANS 50450-1:2011, was supplied by Ulula Ash, South Africa. MK (Grade K40) was obtained from Serina Trading, South Africa. The specific gravities of the precursors are 1.56 and 1.62 for FA and MK, respectively.

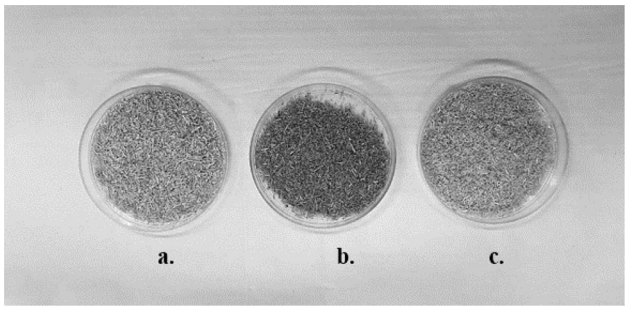

Fig. 1 Particle size of lignocellulosic materials **a** *A. longifolia*, **b** SCB, **c** *A. mearnsii*

2.2 Chemical activators

A combination of sodium silicate and sodium hydroxide at a weight ratio of 2.5:1 based on solid content of materials was used. Sodium silicate, branded as Silchem 2008, with a silica modulus of 2 (29.05% SiO_2 and 14.17% Na_2O) was supplied by PQ Silicas, SA. Analytical grade sodium hydroxide pellets (98% purity) were purchased from Merck Chemicals (Pty) Ltd., SA.

3 Methods

3.1 Characterization of lignocellulosic materials

Compositional analysis to determine the acid-insoluble lignin, sugar contents (glucose, cellobiose, xylose, and arabinose) were conducted according to National Renewable Energy Laboratory (NREL) Analytical Procedure (LAP 013), while TAPPI Standard (T211, 2004) was used to calculate the ash content of the samples. The bulk density of the LM was determined according to the procedures outlined in Miranda et al. (2012).

3.2 Precursors and products characterization

The particle size analysis of FA and MK was carried out using Saturn DigiSizer 5200 V 1.12 operated at a flow rate of 12.0 l/min and ultrasonic intensity of 60%. X-ray fluorescence (XRF) was used to analyse the chemical composition of the precursors. Fourier transform infrared spectroscopy (FTIR) was performed using Thermo Scientific Nicolet iS10 Spectrometer equipped with a Smart iTR attenuated total

reflectance (ATR) accessory to qualify the nature of bonding exhibited by the LM, precursors and the resulting geopolymer-bonded composite products. X-ray diffraction (XRD) was carried out using a Bruker D2 Phaser diffractometer, employing CuKα (λ = 1.5418 Å) at 30 kV and 10 mA. The diffraction intensities were captured with a Lynxeye detector with 2θ scans in the range 4°–50° with a 0.020° step size. Micrographs of the samples were captured and analysed using a Zeiss EVO® MA15 scanning electron microscope (SEM) operated in backscattered electron (BSE) mode.

3.3 Formulation of chemical activator

The weight ratio of precursor material to the activation medium (PA ratio) was set at 2:1 and 3:1. FA was substituted with 25% MK to form a binary precursor material with a Si/Al weight ratio of 1.53. The preparation of a sodium hydroxide solution is an exothermic reaction; hence, it was prepared a day prior to mixing with sodium silicate. The weight ratio of Na_2SiO_3 to NaOH was fixed at 2.5:1. 8 M, 10 M, and 12 M sodium hydroxide solutions were mixed with sodium silicate, yielding activator moduli of 1.27, 1.18 and 1.11, respectively. The PA ratio of 2:1 produced alkali dosages of 10.19, 10.98 and 11.72 with 8 M, 10 M and 12 M NaOH, respectively. The alkali dosages were 6.79, 7.32 and 7.81 for PA ratio of 3:1.

3.4 Experimental design and board formation

Four major factors were considered in this study. These are the curing pattern (CP), PA ratio, molar concentration of NaOH (MConc), and LM type. A mixed factorial experiment based on two factors at 2 levels (CP and PA) and two factors at 3 levels (MCon and LM) with three replicates each was laid out using Statistica 13.3 for the board production. A constant LM content of 25% (oven-dry weight) based on precursor composition was used. The overview of the mix design is presented in Table 1. Untreated LM was mixed with precursor materials in a dry state for 3 min before a predetermined quantity of activator was added and thoroughly mixed for another 5 min. Additional water was added to keep the water/binder ratio (W/B) at 0.28 and mixing was further extended for 2 min. The mixture was transferred into a rectangular mould and cold-pressed at 100 psi for 5 min. The control samples were made with a PA ratio of 2:1, a combination of sodium silicate and 10 M NaOH at a ratio of 2.5:1, and cured at 60 °C for 24 h. The target density (1.10 g/cm^3) was constant for all boards during pouring.

3.5 Curing regimes

Low calcium FA requires heat curing to initiate setting and early strength development of the composites. The boards were cured under two different conditions; a slightly elevated temperature of 60 °C for 24 h and 100 °C for 6 h. The curing technique was carried out according to Chareerat et al. (2006). Prior to heat curing in the oven, the boards were left in room temperature conditions for 1 h. Then, the boards were wrapped with aluminium foil to prevent excessive loss of water during heat treatment. Thereafter, the boards were left in a temperature and humidity-controlled environment for 28 days, after which they were tested for mechanical and physical properties.

3.6 Mechanical and thermal tests

The physical and mechanical properties of the composite boards were evaluated at the age of 28 days, as specified

Table 1 Overview of the mix design for board formation

Runs	FA (g)	MK (g)	LM (g)	Na_2SiO_3 (g)	NaOH (g)	Water (g)	Conc. (M)	Curing pattern (°C, h)
1	120	40	40	57.14	22.86	14	8	60, 24
3	120	40	40	57.14	22.86	15	10	60, 24
5	120	40	40	57.14	22.86	16	12	60, 24
2	135	45	45	42.86	17.14	24	8	60, 24
4	135	45	45	42.86	17.14	26	10	60, 24
6	135	45	45	42.86	17.14	28	12	60, 24
7	120	40	40	57.14	22.86	17	8	100, 6
8	120	40	40	57.14	22.86	17	10	100, 6
9	120	40	40	57.14	22.86	18	12	100, 6
10	135	45	45	42.86	17.14	24	8	100, 6
11	135	45	45	42.86	17.14	26	10	100, 6
12	135	45	45	42.86	17.14	28	12	100, 6
Control	142.50	47.50	–	67.86	27.14	–	10	60, 24

in ASTM D1037-99 (1999). Physical tests included the determination of density, water absorption (WA), thickness and volumetric swelling (TS/VS). The modulus of rupture (MOR) and modulus of elasticity (MOE) were evaluated for mechanical strengths. A 3-point bending test was conducted with an Instron machine fitted with a 5 kN load cell operated at a speed of 5 mm/min. The dimension of the samples for mechanical test was 218 mm × 75 mm × 13 mm, whilst that for sorption test was 75 mm × 50 mm × 13 mm. Thermogravimetric analysis (TGA) to investigate the thermal stability of the composite boards was carried out using a TA Instruments model Q500. The heating was performed under N_2 gas purge (flow rate of 40.0 ml/min) at a ramp rate of 10 °C/min to 600 °C.

4 Results and discussion

4.1 Characterization of LM

Table 2 shows the compositions of the LM used in this study. *A. mearnsii and A. longifolia* had a very similar composition, which was different from SCB. Huang and Qin (2005) also reported similarities in the chemical compositions of other acacia species, such as *A. auriculaeformis, A. crassicarpa,* and *A. mangium. A. mearnsii* had slightly higher lignin, holocellulose, extractives and ash content than *A. longifolia*. This slight difference, however, caused marked differences on some properties of the respective composite products. SCB had higher ash and extractive contents than the acacia species.

4.2 Characterization of precursor materials

The particle size distribution of FA and MK are shown in Table 3. The FA had finer particles than MK, with about 10% of the particles less than 1.383 µm and most of the particles within 10–40 µm. Table 4 shows the composition of the metallic oxides present in the precursors. The FA can be classified as low calcium ash according to the ASTM C618 (ASTM 2019) since the sum of SiO_2 and Al_2O_3 contents exceeded 70% and the CaO content was less than 20%. The precursors met the preferred properties for the production of geopolymer of optimum binding properties outlined in Fernandez-Jimenez et al. (2008). The loss on ignition (LOI) was less than 5%, less than 10% Fe_2O_3, 40–50% SiO_2 and 80–90% of particles less than or equal to 45 µm.

Table 2 Compositional analysis of the LM

Parameters (%)	Lignocellulosic materials		
	A. longifolia	*A. mearnsii*	SCB
Lignin	24.41 (2.52)	23.85 (1.25)	26.84 (2.18)
Hemicellulose	19.05 (0.86)	20.29 (0.11)	10.75 (1.01)
Cellulose	31.54 (0.48)	33.72 (0.13)	23.78 (0.46)
Water extractives	5.51 (0.17)	5.52 (0.75)	9.72 (0.10)
Ethanol extractives	0.54 (0.04)	0.61 (0.09)	1.72 (0.02)
Total extractives	6.08 (0.11)	6.37 (0.58)	11.49 (0.07)
Ash	0.67 (0.02)	0.71 (0.03)	3.99 (0.62)
Moisture content	6.94 (0.09)	7.43 (0.01)	5.90 (0.04)
Bulk density (kg/m^3)	181.43 (5.48)	162.38 (2.59)	119.66 (3.48)

Values in parentheses are standard deviations

Table 3 Particle size distribution and the specific gravity of the precursors

Precursors	Particle size (µm)		
	d_{10}	d_{50}	d_{90}
Fly ash	1.383	14.404	59.804
Metakaolin	2.775	28.052	103.736

4.3 Physical and mechanical properties of geopolymer bonded boards

The apparent density, water absorption (WA), thickness and volumetric swelling (TS/VS) of the boards are shown in Table 5. The samples had comparable densities ranging between 1.12–1.28 g/cm^3, 1.15–1.29 g/cm^3 and 1.00–1.39 g/cm^3 for *A. mearnsii*, *A. longifolia,* and SCB boards, respectively. The boards were categorized as high-density boards as they were above 1.00 g/cm^3 (ANSI 1999). The addition of LM caused a reduction of about 35% in the unit weight of the pure geopolymer boards (Table 5). The unit weights of the boards were lower than the range reported for fly ash-based geopolymer in the literature, i.e. 14.5–15.5 kN/m^3 (Chen et al. 2014), 14.50–17.10 kN/m^3 (Andini et al. 2008) and 11.8–15.7 kN/m^3 (Cioffi et al. 2003). The low unit weight was attributed to the low bulk density of the incorporated LM (Chen et al. 2014).

Following 24 h immersion in water, the WA ranged from 20.33 to 31.53%, 22.37 to 35.99%, and 23.23 to 40.82% for *A. longifolia, A. mearnsii,* and SCB boards, respectively; while the TS ranged from 0.10 to 1.08%, 0.51 to 1.08%, and 0.21 to 2.42% for *A. longifolia, A. mearnsii,* and SCB boards, respectively. Unreinforced geopolymer boards had better sorption properties than the reinforced geopolymers due to the hydrophilic nature of LM. According to EN 634-2:2007 Standard for cement-bonded particleboards, all boards met the TS and VS requirements. However, only a few of the boards from each LM met the WA requirement (Table 5).

Flexural strength, as indicated by the static MOE and bending MOR, is an important requirement for boards used for structural applications in outdoor conditions.

Table 4 Chemical composition of precursor materials

Precursor (%)	Al_2O_3	CaO	Cr_2O_3	Fe_2O_3	K_2O	MgO	MnO	Na_2O	P_2O_5	SiO_2	TiO_2	LOI
Metakaolin	42.24	0.08	0.01	0.39	0.08	–	0.01	0.05	0.07	55.18	1.33	1.02
Fly ash	31.05	5.56	0.01	2.66	0.95	1.18	0.04	0.18	0.44	54.24	1.62	2.00

Table 5 Physical and mechanical properties of the boards and EN 634-2:2007 requirements for cement-bonded particleboards for use in humid and external conditions

Properties	Units	Boards				Standard
		A. mearnsii	*A. longifolia*	SCB	Control[a]	EN 634-2:2007
MOE	MPa	2293–6408	2296–7986	1512–4686	3895 (174)	Class 1: ≥ 4500 Class 2: 4000
MOR	MPa	3.17–7.18	2.77–9.28	1.68–4.95	5.17 (0.03)	≥ 9.0
Density	g/cm^3	1.12–1.28	1.15–1.29	1.00–1.39	1.56 (0.012)	≥ 1.0
Unit weight	kN/m^3	10.98–12.54	11.27–12.64	9.80–13.62	15.29 (0.12)	–
WA	%	22.37–35.99	20.33–31.53	23.23–40.82	10.66 (0.372)	≤ 25
TS	%	0.51–1.08	0.10–1.08	0.21–2.42	0.09 (0.003)	≤ 15
VS	%	0.80–1.68	0.15–1.64	0.21–2.61	0.13 (0.020)	≤ 15

[a]Values in parentheses are standard deviations

The MOE and MOR ranged from 2293 to 6408 MPa and 3.17 to 7.18 MPa, respectively for *A. mearnsii* boards, 2296–7986 MPa and 2.77–9.228 MPa for *A. longifolia* boards and 1512–4686 MPa and 1.68–4.95 MPa for SCB boards. The addition of wood particles of acacia species improved the flexural strength of the boards. The boards had comparable flexural properties with fly ash and steel slag-based geopolymer reinforced with synthetic fibres reported by Guo and Pan (2018). SCB fibres only slightly improved the MOE and caused a reduction in the MOR of the boards compared to the control. This is due to the low bulk density of the SCB and the high volume included in the matrix. However, the boards had better flexural strength than those reported by Amiandamhen et al. (2018b) using similar wood species in phosphate matrix. The boards produced also performed better than those reported by Chen et al. (2014) using sorghum fibres in fly ash-based geopolymer. The flexural strength compares well with the results of Duan et al. (2016), where sawdust content of 20% showed maximum flexural strength of about 10 MPa and 12 MPa after 28 and 90 days curing, respectively. According to EN 634-2:2007, there are two classes of boards based on the static MOE (Class 1 and Class 2) and a minimum MOR of 9 MPa is required for each class (Table 5). Within the experimental conditions in this study, only *A. longifolia* boards met all the minimum requirements.

4.4 Effect of curing pattern and LM on physical properties

Increasing the curing temperature up to 100 °C has been reported to have positive effects on the properties of geopolymer products (Yuan et al. 2016). Figure 2a shows that there is a significant difference between the curing patterns employed in this study. Boards cured at 60 °C had a higher mean density than those cured at 100 °C. This observation is in agreement with findings in the literature (Sarmin and Welling 2015; Tran et al. 2009). The authors reported a reduction in the density of geopolymers as the curing temperature increased. Curing beyond 100 °C caused the formation of numerous cavities resulting in decreased density and strength. However, Fig. 2b shows that the trend varied with different LM. Curing at 100 °C for 6 h resulted in a slightly higher mean density than 60 °C curing for both *A. longifolia* and *A. mearnsii* boards. Statistical analysis ($p < 0.05$) revealed that the curing pattern had no significant effect on the density of boards for both species, which indicates that the two curing conditions employed in this study did not deteriorate the internal structure of the acacia boards. In contrast, curing at 100 °C for 6 h caused a reduction in the density of SCB boards by about 15.59%. SCB has a low bulk density, which implies that more particles and embodied moisture were incorporated in SCB boards than the other board types. Higher curing temperature causes the formation of micro cracks (Görhan et al. 2016), increases the extent of dehydroxylation between T–OH (T: Si or Al) and rate of removal of both free water and pore water resulting in the formation of large voids (Yuan et al. 2016). The formation of large voids was further accentuated by the reduced compressibility (due to high volume) which caused the board volume to expand, leading to a reduction in board density. An increase in composite volume due to the formation of cavities, as a result of rapid moisture removal at higher temperatures was also reported by Tran et al. (2009). Statistical analysis ($p < 0.05$) revealed a significant effect of curing conditions on the density of SCB boards (Fig. 2b).

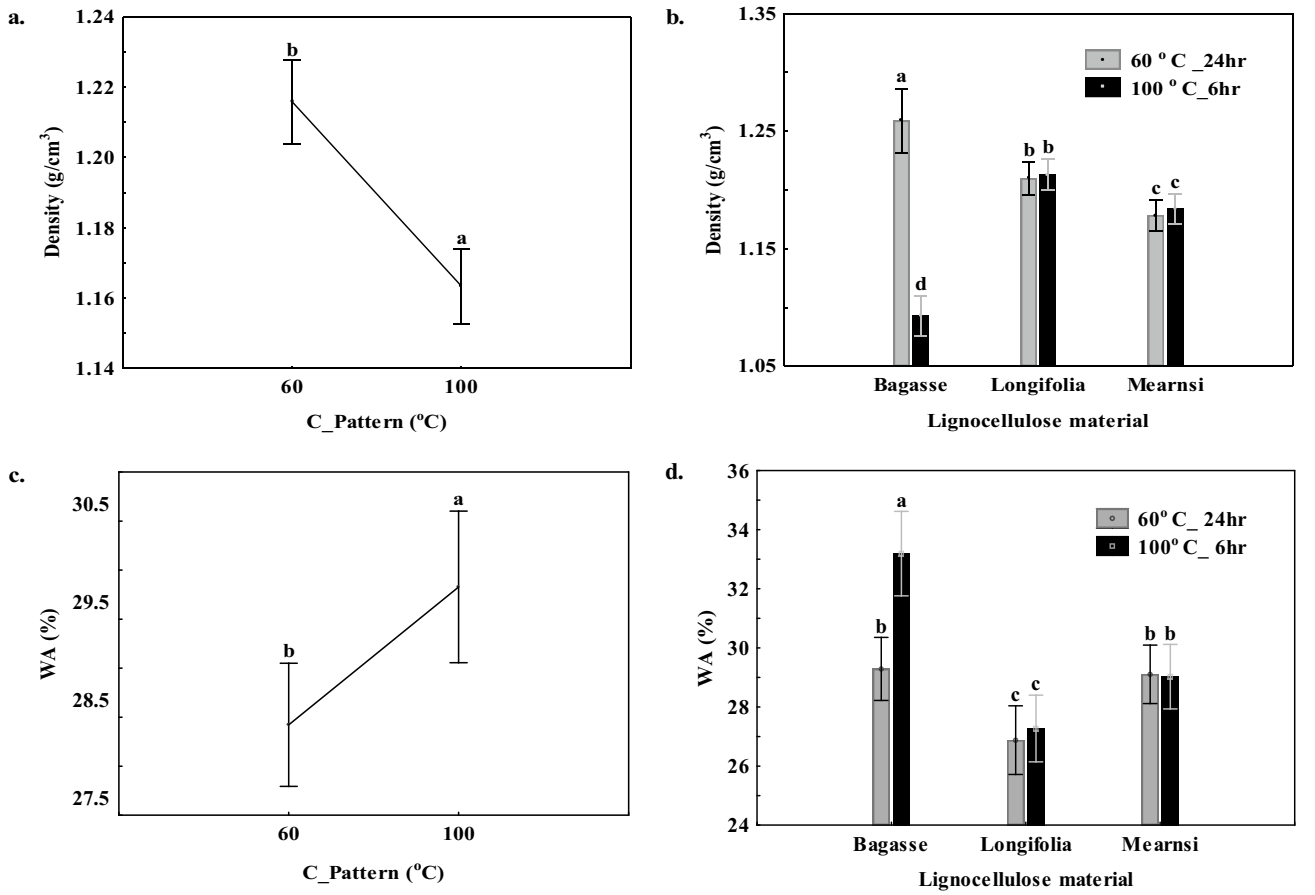

Fig. 2 Effects of curing pattern—on board density **a** for all boards, **b** for each LM;—and water absorption **c** for all boards **d** for each LM. *Factors with the same letters are not significantly different from each other ($p < 0.05$)

Generally, boards cured at 100 °C for 6 h absorbed more water and there was no significant difference between curing conditions and TS/VS. However, the influence was different for different LM (Figs. 2 and 3). The effects on the sorption properties of SCB boards followed the same trend as density. Boards cured at 60 °C for 24 h absorbed less water and had better dimensional stability than those cured at 100 °C for 6 h. This can be explained by the fact that the porous morphology due to high-temperature curing exposed more sorption sites on the SCB fibre and the matrix was not compact enough (due to lower compressibility at high fibre loading) to resist the dimensional changes associated with water uptake. The curing pattern had significant effects ($p < 0.05$) on the WA, TS, and VS of SCB boards. *A. longifolia* boards cured at 60 °C for 24 h had a lower mean WA but were less dimensionally stable compared with those cured at 100 °C for 6 h, as they had higher mean TS/VS values. The formation of micro cracks and cavities at elevated temperatures provided more channels for water molecules to penetrate the boards (See Fig. 4a). However, the lower TS/VS at 100 °C curing is evidence that the water was only absorbed into the open cracks and the matrix was compact enough to uphold the dimensional integrity of the boards. Curing patterns had a significant effect on TS and VS for *A. longifolia* boards but their influence on WA was insignificant ($p > 0.05$). *A. mearnsii* boards behaved differently: boards cured at 60 °C for 24 h absorbed more water and had higher mean TS but lower VS values than those cured at 100 °C for 6 h. The disparity could be as a result of the difference in the cellular and chemical composition of the species. Statistical analysis revealed no significant influence of curing pattern on the sorption properties of *A. mearnsii* boards.

4.5 Effect of PA ratio and activator concentration on board properties

The effects of PA ratio and activator concentration on the physical and mechanical properties of the boards are presented in Figs. 5 and 6, respectively. The PA ratio and activator concentration are critical factors, which greatly influence the formation and evolution of the overall strength of geopolymer products (Petermann et al. 2010). While keeping

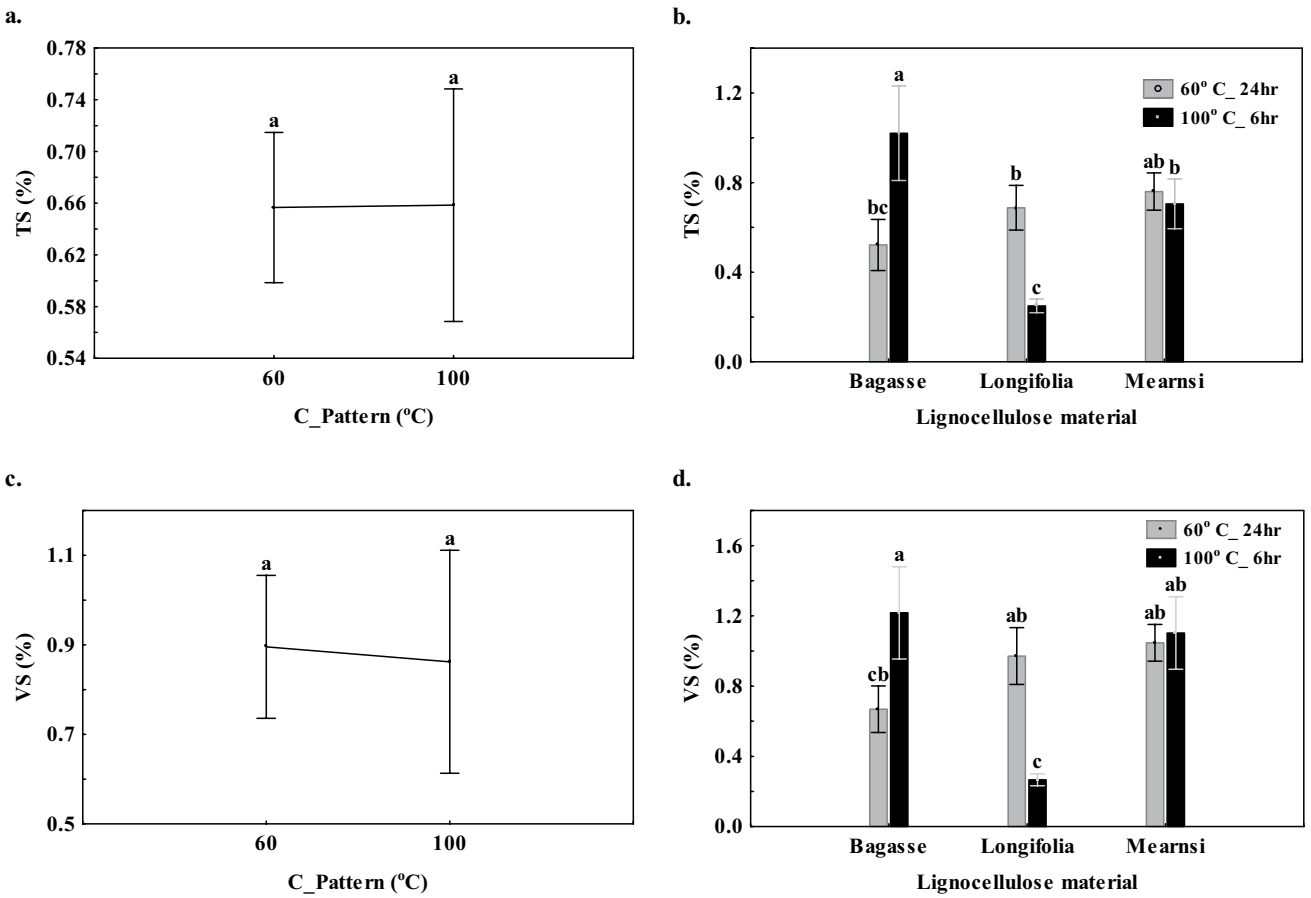

Fig. 3 Effects of curing pattern on TS—**a** for all boards, **b** for each LM;—and VS **c** for all boards, **d** for each LM

the weight ratio of Na_2SiO_3 and NaOH fixed at 2.5:1, the PA ratio of 2:1 produced alkali dosage (%Na_2O/binder) of 10.19, 10.98 and 11.72% with 8 M, 10 M and 12 M NaOH, respectively; compared to the dosages of 6.79, 7.32 and 7.81% recorded for PA ratio of 3:1. Irrespective of LM type and activator concentration, a PA ratio of 2:1 had higher mean density, MOE, MOR and lower WA than a PA ratio of 3:1. The improved properties are due to the higher alkali dosage, which enhanced the dissolution stage of the geopolymerization kinetics and subsequently aided the densification of the pore structure as seen in Fig. 4b.

The effect of alkali dosage on the strength development of geopolymers has been reported in the literature. According to Soutsos et al. (2016), increasing the alkali dosage affected the properties of fly ash-based geopolymers until an optimum value of 12.5%, beyond which the strength decreased. The alkali dosages used in this experiment were below this optimum value. The MOE and MOR of acacia boards improved as the molar concentration of the activator increased. There is an exception with SCB boards where the strength properties decreased when the molar concentration increased from 10 to 12 M. This could be explained by the presence of high extractive content and lignin in SCB which leached and retarded the dissolution of both silica and alumina species and delayed the nucleation stage of geopolymer synthesis. This might have caused migration of excess alkali anions into the fibre bundles leading to degradation of the holocellulose. This is in line with the result of Ye et al. (2018) that higher lignin content caused reduction in the strength of metakaolin-based geopolymer.

4.6 Effects of curing pattern and LM on mechanical properties of boards

Figure 7 shows the effect of curing pattern on the strength properties of the boards. The effects followed the same trend as was observed with the board density for all LM. SCB boards cured at 60 °C for 24 h had higher mean MOE and MOR than those cured at 100 °C for 6 h, while the reverse was observed with acacia boards. Figure 8 shows weak positive correlations observed between board density and the strength properties. Amiandamhen et al. (2018b) reported a similar observation in phosphate bonded composites where invasive acacia wood was incorporated in the matrix as

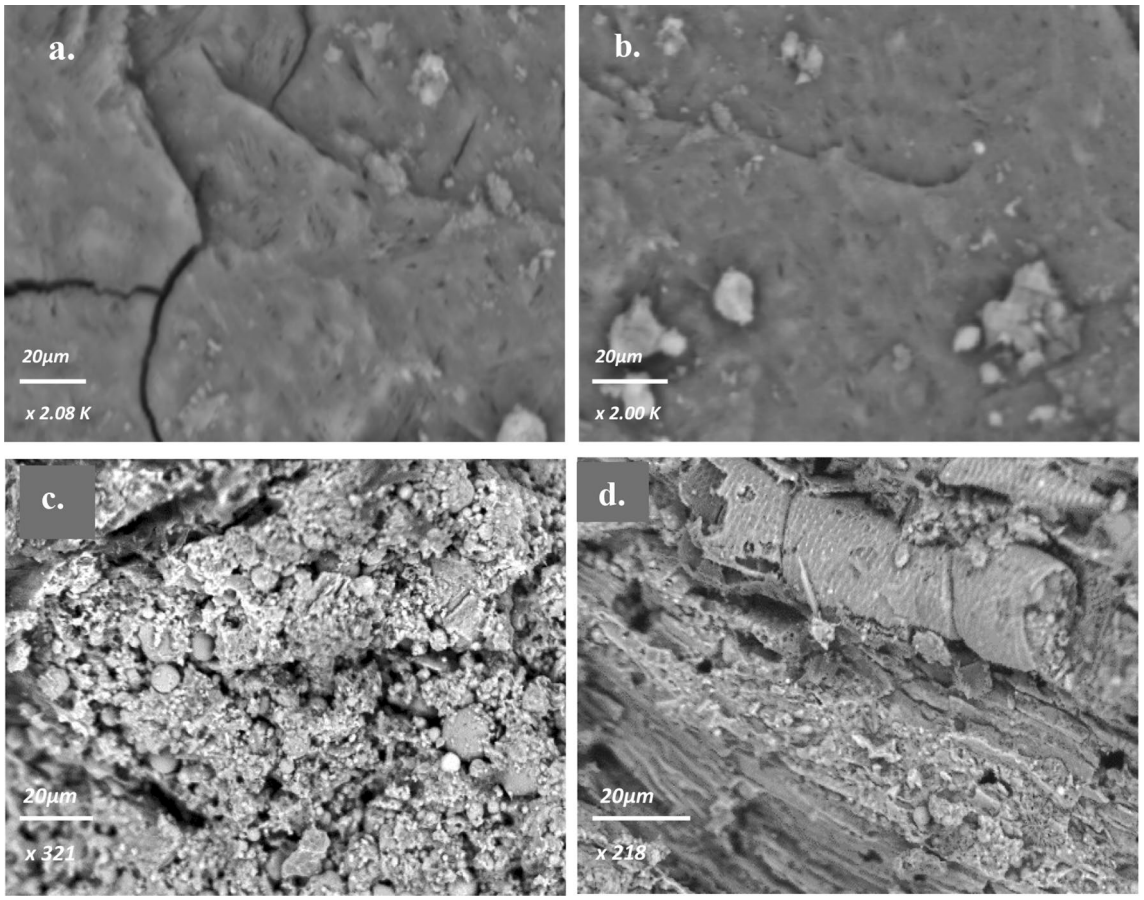

Fig. 4 SEM micrographs showing **a** formation of microcracks and channels at high temperature curing in *A. longifolia* board, **b** densified pore structure, **c** fractured surface of SCB board, **d** mineralized fibres of *A. mearnsii* boards

reinforcement. Irrespective of LM, the curing pattern had significant effects ($p < 0.05$) on the strength properties of the boards with the exception of the MOE of SCB boards. Curing at 100 °C for 6 h accelerated the geopolymer kinetics and improved the strength properties of acacia boards. Increasing the curing temperature up to 100 °C has been reported to improve the strength development of low-calcium fly ash (Class F) geopolymers, regardless of the curing duration (Hardjito and Rangan 2005).

A. mearnsii boards cured at 60 °C for 24 h had a higher mean MOE and MOR than *A. longifolia* boards cured at the same temperature, which could be due to its slightly higher cellulose content. Higher cellulose content improves the strength properties of geopolymers as the bridging mechanism of the fibres impedes crack propagation (Ye et al. 2018). However, the trend was reversed when the curing temperature was raised to 100 °C for 6 h. *A. longifolia* boards recorded a significant strength gain compared to *A. mearnsii* boards (Fig. 7). This could be due to the slightly higher hemicellulose content in *A. mearnsii*, which can degrade in an alkaline environment at higher temperature curing. The SEM image (Fig. 4d) shows that the fibres in *A. mearnsii* boards were mineralized, as the geopolymer matrix can be seen absorbed into the fibre bundles. This caused degradation of hemicelluloses, which was further confirmed by FTIR results. The degraded hemicelluloses in the alkaline matrix, together with the high extractive content, could cause a reduction in the geopolymerization kinetics.

4.7 Characterization of the geopolymer product

4.7.1 FTIR

The infrared (IR) spectra of the precursor materials are shown in Fig. 9. Fly ash has more peaks than metakaolin, but it is important to note that the peaks fall within the same band areas. The band between 950 and 1250 cm^{-1} is assigned to the internal vibrations of Si–O–Si (Davidovits 2008). They also have peaks in the band 500–800 cm^{-1} which is characteristic of symmetric stretching of the Si–O–Si and Al–O–Si bonds of amorphous or semi-crystalline alumino-silicates (Barbosa et al. 2000; Fauzi et al.

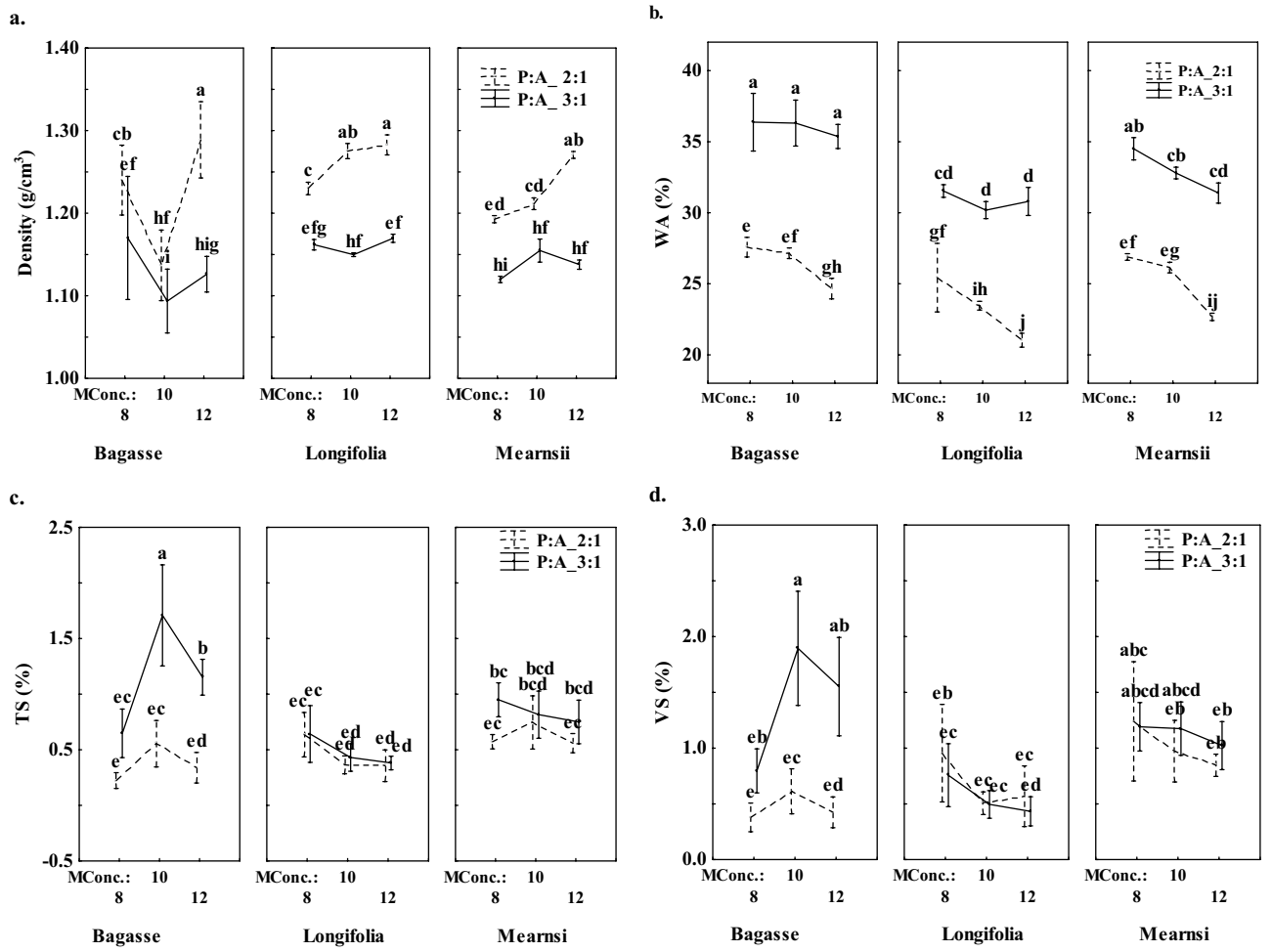

Fig. 5 Effects of PA ratio and molar concentration on **a** board density, **b** WA, **c** TS, **d** VS

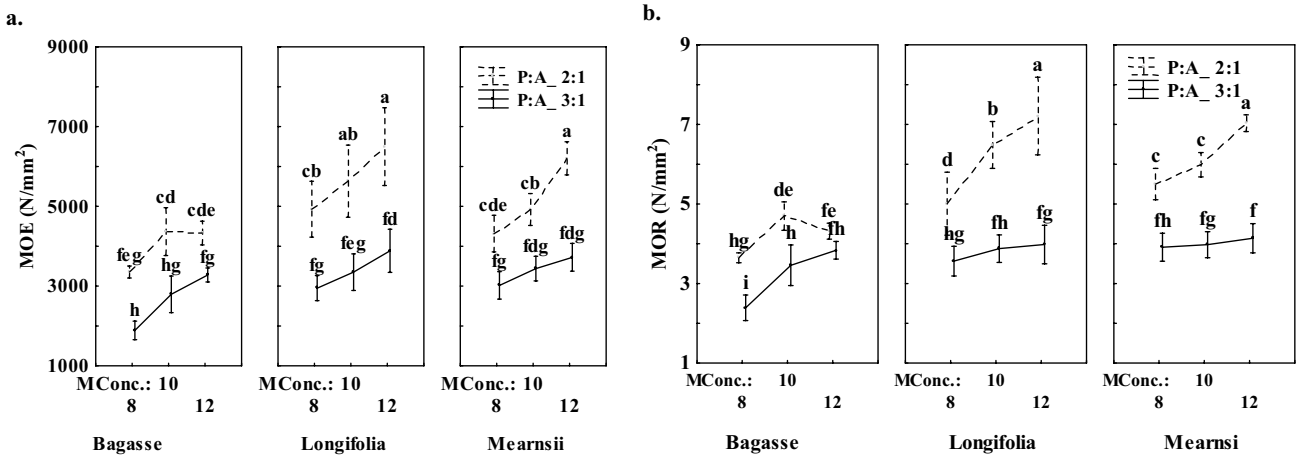

Fig. 6 Effects of PA ratio and activator concentration on MOE and MOR

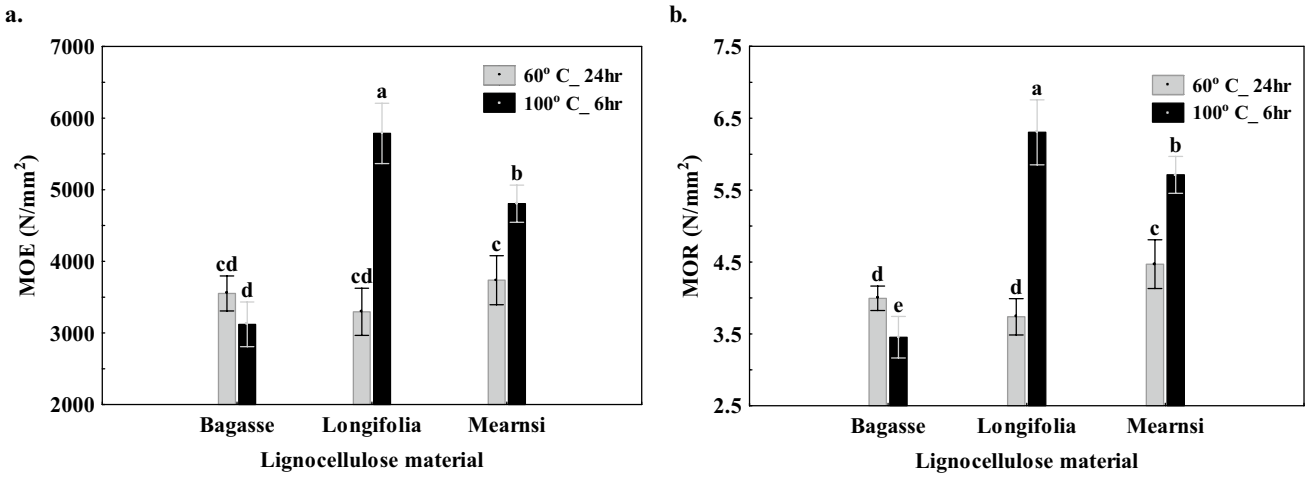

Fig. 7 Effects of curing pattern on **a** MOE, **b** MOR

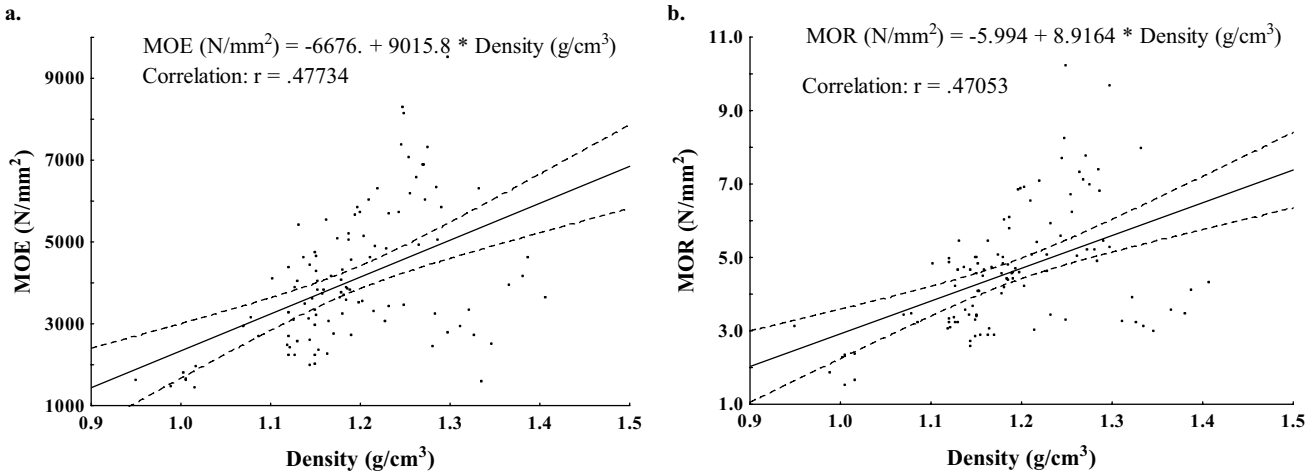

Fig. 8 Relationship between density and **a** MOE, **b** MOR

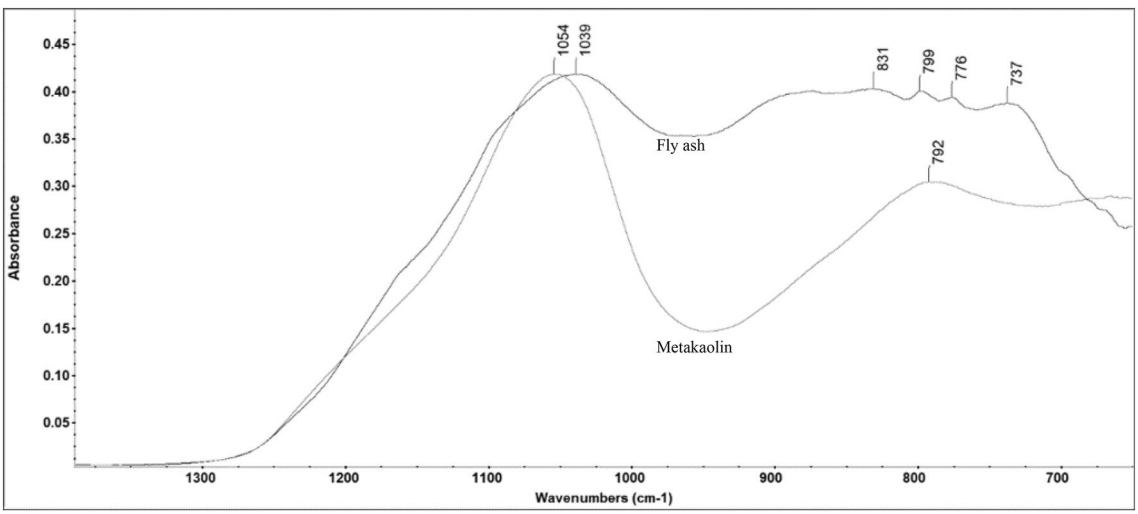

Fig. 9 FTIR spectra of precursor materials

2016). The LM types have similar IR spectra within the same band numbers as shown in Fig. 10a. The strongest bands are found around 3360 cm^{-1} and 1023 cm^{-1} in all LM samples. The band around 3360 cm^{-1} is assigned to the axial vibration of the hydroxyl (–OH) group of cellulose (Ibraheem et al. 2016), while the band at 1023 cm^{-1} indicates a C–C bond of β-glucosidic linkages between sugar units in hemicelluloses and cellulose (Hajiha et al. 2014). The peak at 2916 cm^{-1} represents a symmetrical vibration of C–H bond (Liu et al. 2004; Amiandamhen et al. 2018a). Since the SCB fibre has been processed, it could have altered the position of the absorption bands. This peak could also be attributed to a C–H aliphatic axial deformation in CH_2 and CH_3 groups from cellulose, lignin and hemicellulose as it is only 4 cm^{-1} less than the absorption band reported by Corrales et al. (2012). The peak around 1737 cm^{-1} is attributed to the carbonyl (C=O) stretching of acetyl groups of hemicellulose (Liu et al. 2004; Corrales et al. 2012). These peaks disappeared in the IR spectra of their respective boards (Fig. 10b), indicating the degradation of hemicelluloses in the matrix. SCB has peaks at 1603 cm^{-1} and 1633 cm^{-1}, which could be assigned to C-Ph vibration at peak and C=C bonds found in lignin aromatic structures (Corrales et al. 2012). The C-Ph peak disappeared in SCB boards.

The peak at 1422 cm^{-1} is present in both SCB and the acacia species, indicating CH_2 symmetric bending of cellulose (Hajiha et al. 2014; Sawpan et al. 2011). The peak shifted to around 1416 cm^{-1} and the intensity decreased in the geopolymer products, indicating the partial degradation of lower molecular cellulose components. The C–O stretch of the acetyl group of lignin assigned to the peaks found around 1235–1254 cm^{-1} (Hajiha et al. 2014; Liu et al. 2004) also disappeared in the composite products.

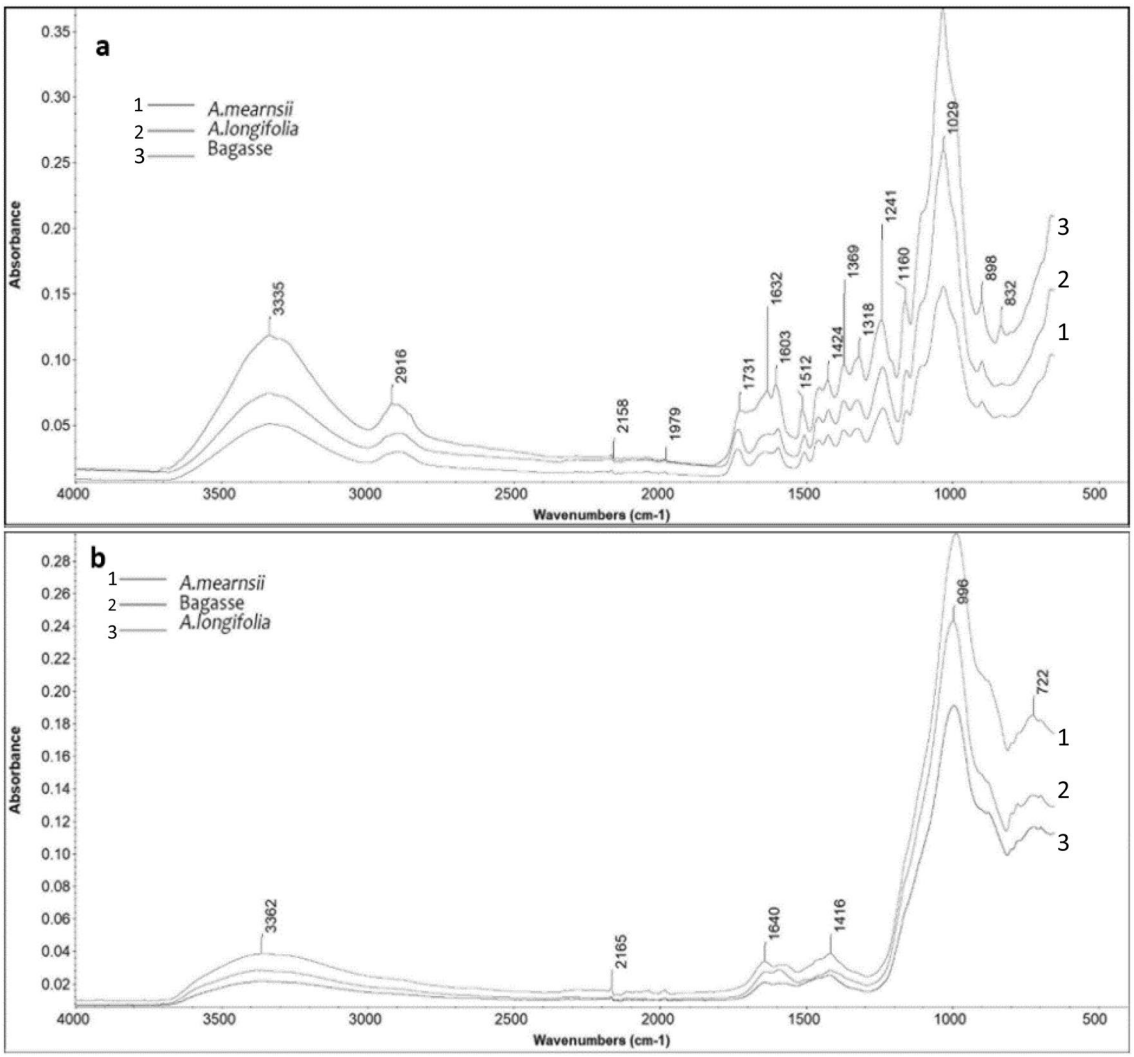

Fig. 10 FTIR spectra of **a** LMs, **b** composite products after 28 days

This indicates a partial breakdown of lignin in the alkaline matrix. The major peak found in the geopolymer products is due to the convolution shifts of the Si–O–Si band of the precursor materials (Fig. 10) and the C–C peak of the LM towards the low wavenumber (Fig. 10b). The shift in the Si–O–Si and Al–O bands towards lower wavenumber indicates that geopolymerization has occurred through partial replacement of silica species by alumina, resulting in a change in the local chemical environment of the bonds (Criado et al. 2005; Davidovits 2008).

4.7.2 TGA

The thermal stability of the LM and composite products was investigated by thermogravimetric analysis (TGA) under nitrogen flow. The derivative thermograms (DTG) of the LM are shown in Fig. 11. The LMs exhibited similar thermal behaviour to the presence of peak/shoulders below the main degradation peak. The shoulders appeared at 272.43 °C, 274.70 °C and 293.49 °C for *A. mearnsii, A. longifolia* and SCB, respectively. The shoulder may be attributed to the degradation of hemicelluloses partially overlapping with cellulose and lignin (Sebio-Puñal et al. 2012). *A. mearnsii* has another shoulder at 225.12 °C, which could indicate the decomposition of some volatile components and hemicelluloses of lower molecular weights. The DTG plot of the boards is shown in Fig. 12. The peak-shoulder disappeared in all boards, which corroborates the FTIR results that the hemicellulose components have degraded in the alkaline matrix. The shift in the main degradation peaks towards the lower end of the cellulose degradation range of 275–500 °C also confirms the partial degradation of cellulose and lignin (Machado et al. 2018). Other broad peaks found around 425–525 °C for *A. mearnsii* and *A. longifolia* could indicate an overlap of lignin degradation and transformation of the amorphous matrix contents into a more crystalline structure. This peak is absent in the SCB board, but its weight loss was increasing until it became steady around 540 °C. The products are thermally stable as the residues are all above 70%.

4.7.3 XRD analysis

The XRD diffractograms of fly ash and metakaolin are shown in Fig. 13a. The high hump observed between 15° and 35° 2θ indicates a high level of amorphous content, which could be silica or alumina. Quartz (00-901-0145) and mullite

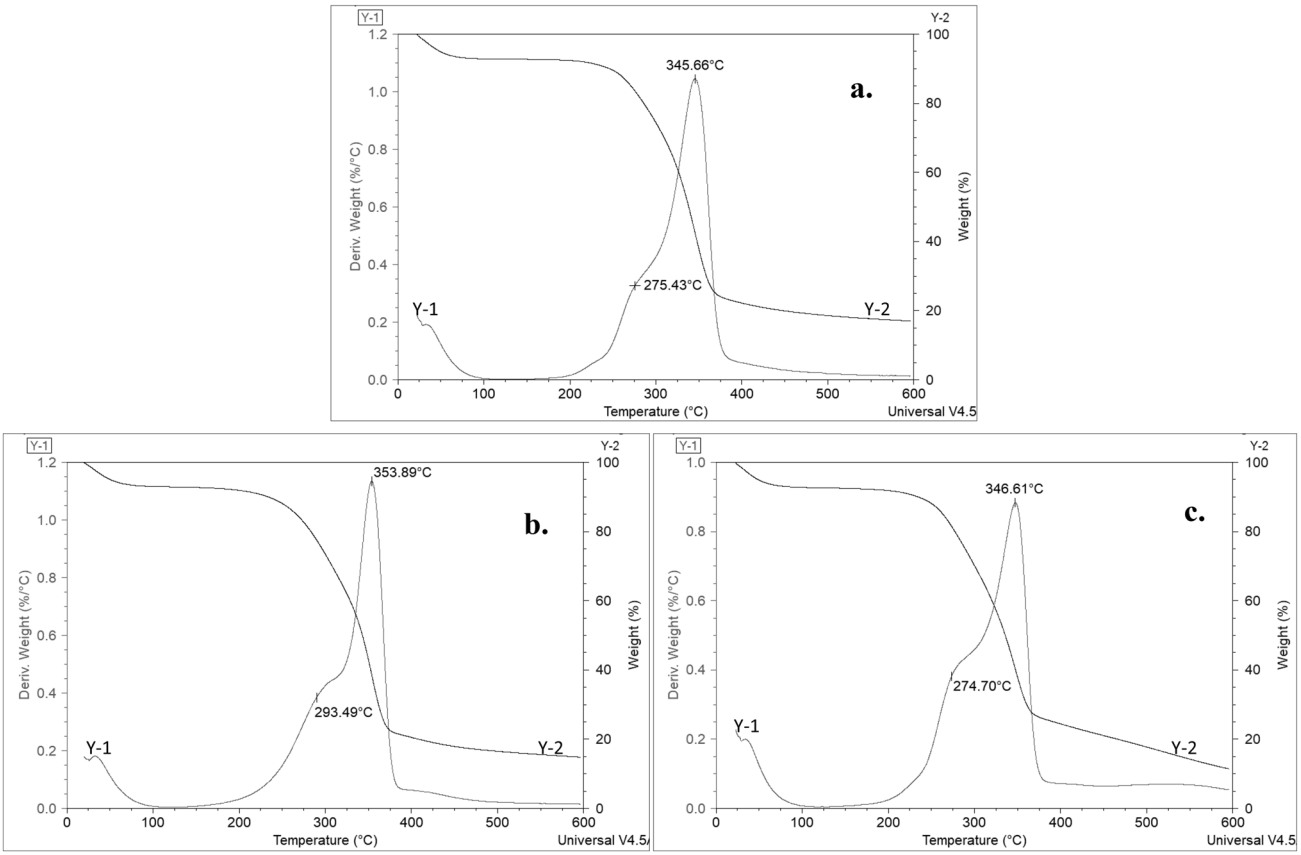

Fig. 11 Thermograms (TG) and derivative thermograms (DTG) of LM: **a** *A. mearnsii*, **b** SCB, **c** *A. longifolia*

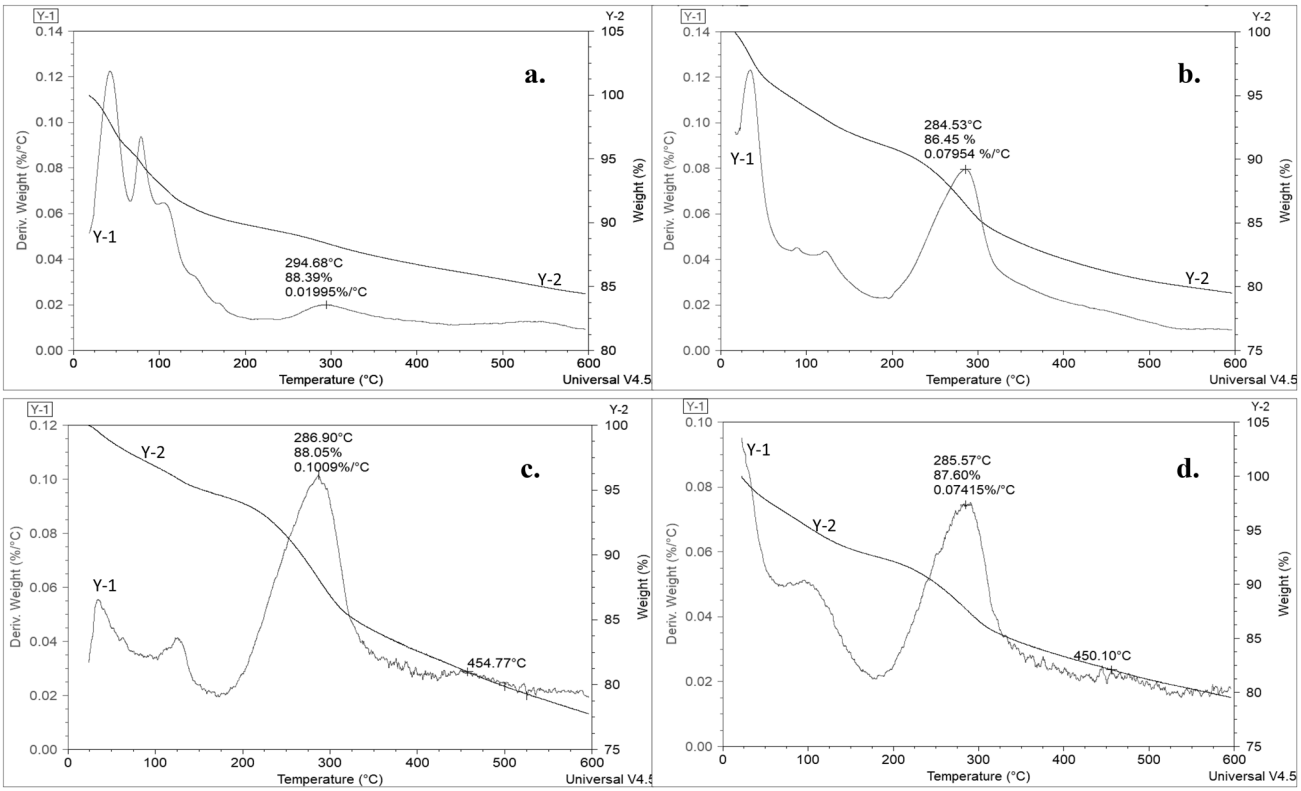

Fig. 12 Derivative and weight loss thermograms of **a** control sample, **b** SCB boards, **c** *A. longifolia* boards, **d** *A. mearnsii* boards

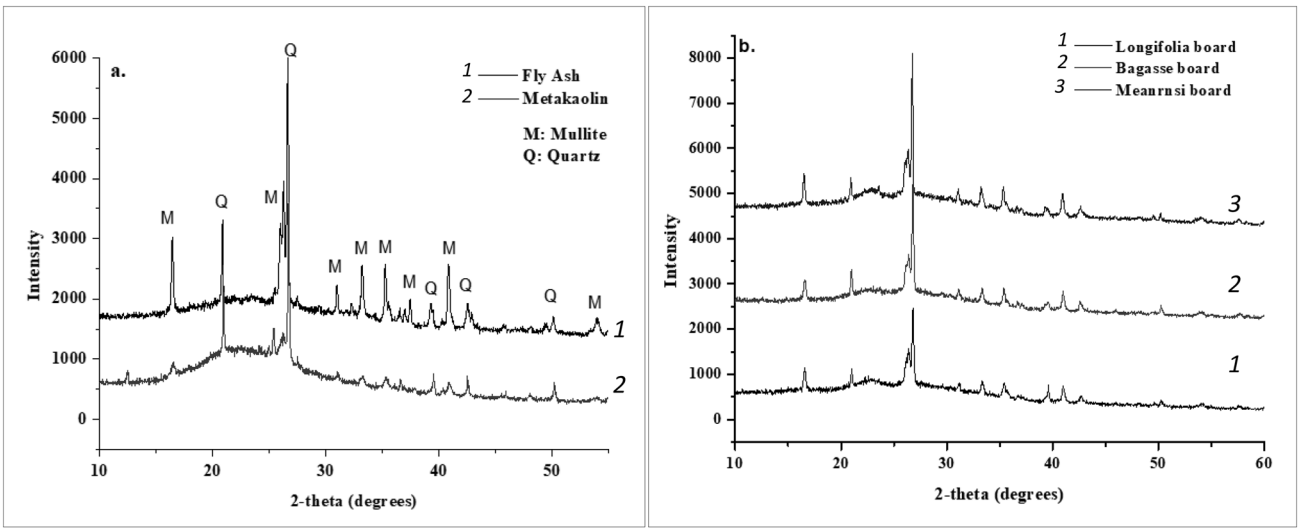

Fig. 13 XRD patterns of **a** precursor materials, **b** geopolymer composites

(00-900-5502) are the principal crystalline phases present in both materials, but their intensities are higher in fly ash than metakaolin. No formation of new crystalline phases was observed in the diffractograms of the composite products shown in Fig. 13b, but the intensity of the identified crystalline phases reduced, and the peak shifted towards higher 2θ values. The shift confirms the FTIR results that geopolymerization has taken place (Yuan et al. 2016), and the reduction in intensity indicates that some parts of the crystalline material took part in the reaction (Alomayri 2017). Fewer crystalline phases participated in the geopolymerization reaction of *A. mearnsii* boards as they exhibit higher

intensities than those found in the other boards (Fig. 13b). *A. longifolia* and *A. mearnsii* had comparable chemical composition (see Table 1), but the difference in the intensities of the crystalline phases in SCB and *A. longifolia* boards are not noticeable, which could mean that *A. mearnsii* contains components that inhibited geopolymerization kinetics.

5 Conclusion

This study has demonstrated the possibility of producing high-density geopolymer panels reinforced with untreated wood particles from South African invasive species and SCB for use in outdoor conditions. The following conclusions can be drawn based on this study:

1. Curing pattern, molar concentration of activator and PA ratio have significant effects on the properties of the geopolymer boards.
2. Increasing the molar concentration of activator and curing temperature results in a denser pore structure and improves the properties of acacia boards. The internal structure of SCB boards deteriorated at higher curing temperature causing low strength development.
3. All geopolymer boards met the sorption requirements of EN 634-2: 2007 for cement-bonded particleboards for outdoor applications. However, only *A. longifolia* boards produced with 12 M NaOH, PA ratio of 2:1 and cured at 100 °C for 6 h met the mechanical strength requirements.
4. The boards are thermally stable, as the residue retained at the end of thermal analysis was above 70%.
5. The products have comparable properties to other natural fibre reinforced composites and can be used as alternative materials in similar applications. The development of geopolymer products utilizing industrial residues presents both economic and environmental advantages when compared to conventional composite products. However, there is a concern about the durability of the LM in alkaline matrix. Mineralization of LM due to high dosage of alkali activator was revealed by SEM, while degradation of hemicellulose and lower molecular wood components was confirmed by FTIR analysis. The degraded products do not prevent geopolymer setting but lower the degree of geopolymerization. Hence, the durability of the product over time needs to be further investigated.

Acknowledgements The authors would like to thank the German Academic Exchange (DAAD) and DLR for funding this study under the BioHome Project in collaboration with the University of Hamburg, Germany and Addis Ababa Institute of Technology, Ethiopia.

Funding The research was done in the BioHome Project funded by the German Federal Ministry of Education and Research [Grant Number: 01DG17007A] and the DAAD Project [Grant Number: 57359374].

Compliance with ethical standards

Conflict of interest The authors declare that they have no conflict of interests.

References

Alomayri T (2017) Effect of glass microfibre addition on the mechanical performances of fly ash-based geopolymer composites. J Asian Ceram Soc 5:334–340. https://doi.org/10.1016/j.jascer.2017.06.007

Alomayri T, Shaikh FUA, Low IM (2013) Characterisation of cotton fibre-reinforced geopolymer composites. Compos Part B Eng 50:1–6. https://doi.org/10.1016/j.compositesb.2013.01.013

Alomayri T, Vickers L, Shaikh FUA, Low IM (2014) Mechanical properties of cotton fabric reinforced geopolymer composites at 200-1000 C. J Adv Ceram 3:184–193. https://doi.org/10.1007/s40145-014-0109-x

Amiandamhen SO, Meincken M, Tyhoda L (2016) Magnesium based phosphate cement binder for composite panels: a response surface methodology for optimisation of processing variables in boards produced from agricultural and wood processing industrial residues. Ind Crops Prod 94:746–754. https://doi.org/10.1016/j.indcrop.2016.09.051

Amiandamhen SO, Meincken M, Tyhoda L (2018a) The effect of chemical treatments of natural fibres on the properties of phosphate-bonded composite products. Wood Sci Technol 52:653–675. https://doi.org/10.1007/s00226-018-0999-9

Amiandamhen SO, Montecuccoli Z, Meincken M, Barbu MC, Tyhoda L (2018b) Phosphate bonded wood composite products from invasive Acacia trees occurring on the Cape Coastal plains of South Africa. Eur J Wood Prod 76:437–444. https://doi.org/10.1007/s00107-017-1191-x

Amiandamhen SO, Meincken M, Tyhoda L (2019) Phosphate bonded natural fibre composites: a state of the art assessment. SN Appl Sci 1:1–10. https://doi.org/10.1007/s42452-019-0910-9

Andini S, Cioffi R, Colangelo F et al (2008) Coal fly ash as raw material for the manufacture of geopolymer-based products. Waste Manag. https://doi.org/10.1016/j.wasman.2007.02.001

ANSI (1999) A208.1-1999, Particleboard, American National Standard, Composite Panel Association, Gaithersburg

ASTM (1999) ASTM D1037-99, standard test methods for evaluating properties of wood-base fiber and particle panel materials, ASTM International. Annu B ASTM Stand. https://doi.org/10.1520/D1037-99

ASTM (2019) ASTM C618-19, standard specification for coal fly ash and raw or calcined natural pozzolan for use in concrete. Annu B ASTM Stand. https://doi.org/10.1520/C0618-19

Barbosa VFF, Mackenzie KJD, Thaumaturgo C (2000) Synthesis and characterisation of materials based on inorganic polymers of alumina and silica: sodium polysialate polymers. Int J Inorg Mater 2:309–317

Buchwald A, Hilbig H, Kaps C (2007) Alkali-Activated metakolin-slag blends—performance and structure in dependance of their composition. J Mater Sci 42:3024–3032

Castaldelli VN, Moraes JCB, Akasaki JL et al (2016) Study of the binary system fly ash/sugarcane bagasse ash (FA/SCBA) in SiO_2/K_2O alkali-activated binders. Fuel 174:307–316. https://doi.org/10.1016/j.fuel.2016.02.020

Chareerat T, Lee-Anansaksiri A, Chindaprasirt P (2006) Synthesis of high calcium fly ash and calcined kaoline geopolymer mortar. In: International conference on pozzolan, concrete and geopolymer. Khhon Kaen, Thailand, p May 24–25

Chen R (2014) Bio Stabilization for Geopolymer Enhancement and Mine Tailings Dust Control. Dissertation. University of Arizona

Chen R, Ahmari S, Zhang L (2014) Utilization of sweet sorghum fiber to reinforce fly ash-based geopolymer. J Mater Sci 49:2548–2558. https://doi.org/10.1007/s10853-013-7950-0

Chimphango A (2020) The valorisation of paper sludge for green composite material. M.Sc. Dissertation. Stellenbosch University

Cioffi R, Maffucci L, Santoro L (2003) Optimization of geopolymer synthesis by calcination and polycondensation of a kaolinitic residue. Resour Conserv Recycl 40(1):27–38. https://doi.org/10.1016/S0921-3449(03)00023-5

Corrales RCNR, Mendes FMT, Perrone CC et al (2012) Structural evaluation of sugar cane bagasse steam pretreated in the presence of CO_2 and SO_2. Biotechnol Biofuels 5:36. https://doi.org/10.1186/1754-6834-5-36

Criado M, Palomo A, Fernández-Jiménez A (2005) Alkali activation of fly ashes. Part 1: effect of curing conditions on the carbonation of the reaction products. Fuel 84:2048–2054. https://doi.org/10.1016/j.fuel.2005.03.030

Davidovits J (2008) Geopolymer chemistry and applications, 3rd edn. Institute Geopolymere, Saint-Quentin

DEA (Department of Environment Affairs) (2012) National Waste information baseline report. Department of Environmental Affairs, Pretoria

Duan P, Yan C, Zhou W, Luo W (2016) Fresh properties, mechanical strength and microstructure of fly ash geopolymer paste reinforced with sawdust. Constr Build Mater 111:600–610. https://doi.org/10.1016/j.conbuildmat.2016.02.091

Fauzi A, Fadhil M, Malkawi AB et al (2016) Study of fly ash characterization as a cementitious material. Procedia Eng 148:487–493. https://doi.org/10.1016/j.proeng.2016.06.535

Fernandez-Jimenez A, Monzo M, Vicent M, Barba A, Palomo A (2008) Alkaline activation of metakaolin-fly ash mixtures: obtain of zeoceramics and zeocements. Microporous Mesoporous Mater 108:41–49

Görhan G, Aslaner R, Şinik O (2016) The effect of curing on the properties of metakaolin and fly ash-based geopolymer paste. Compos Part B Eng 97:329–335. https://doi.org/10.1016/j.compositesb.2016.05.019

Guo X, Pan X (2018) Mechanical properties and mechanisms of fiber reinforced fly ash–steel slag based geopolymer mortar. Constr Build Mater 179:633–641. https://doi.org/10.1016/j.conbuildmat.2018.05.198

Habert G, D'Espinose De Lacaillerie JB, Roussel N (2011) An environmental evaluation of geopolymer based concrete production: reviewing current research trends. J Clean Prod 19:1229–1238. https://doi.org/10.1016/j.jclepro.2011.03.012

Hajiha H, Sain M, Mei LH (2014) Modification and characterization of hemp and sisal fibers modification and characterization of hemp and sisal fibers. J Nat Fibers 11:144–168. https://doi.org/10.1080/15440478.2013.861779

Hardjito D, Rangan BV (2005) Development and properties of low-calcium fly ash-based geopolymer concrete. Research report GC1, Curtin University of Technology, Perth, Australia

Herrmann A, Nickel J, Riedel U (1998) Construction materials based upon biologically renewable resources—from components to finished parts. Polym Degrad Stab 59:251–261

Huang LH, Qin TF (2005) Study on the difference of chemical properties among five acacia species. Forest Research 18(2):191–194. http://europepmc.org/abstract/CBA/520748. Accessed 13 Nov 2020

Ibraheem SA, Sreenivasan SS, Abdan K et al (2016) The effects of combined chemical treatments on the mechanical properties of three grades of sisal. BioResources 11:8968–8980

Kong DLY, Sanjayan JG (2008) Damage behavior of geopolymer composites exposed to elevated temperatures. Cem Concr Compos 30:986–991. https://doi.org/10.1016/j.cemconcomp.2008.08.001

Korniejenko K, Mikuła J, Łach M (2015) Fly ash based fiber-reinforced geopolymer composites as the environmental friendly alternative to cementitious materials. In: Proceedings of 2015 international conference on bio-medical engineering and environmental technology (BMEET 2015). London, March, 21–22, 2015, pp 164–171

Le Maitre DC, Versfeld DB, Chapman R (2000) The impact of invading alien plants on surface water resources in South Africa: a preliminary assessment. Water SA 26:397–408

Le Quéré C, Andrew RM, Friedlingstein P et al (2018) Global carbon budget 2017. Earth Syst Sci Data 10:405–448. https://doi.org/10.5194/essd-10-405-2018

Li Z, Wang X, Wang L (2006) Properties of hemp fibre reinforced concrete composites. Compos Part A Appl Sci Manuf 37:497–505. https://doi.org/10.1016/j.compositesa.2005.01.032

Liu W, Mohanty AK, Askeland P et al (2004) Influence of fiber surface treatment on properties of Indian grass fiber reinforced soy protein based biocomposites. Polymer (Guildf) 45:7589–7596. https://doi.org/10.1016/j.polymer.2004.09.009

Machado G, Santos F, Faria D et al (2018) Characterization and potential evaluation of residues from the sugarcane industry of Rio Grande do Sul in biorefinery processes. Nat Resour 9(5):175–187. https://doi.org/10.4236/nr.2018.95011

Mellado A, Catalán C, Bouzón N et al (2014) Carbon footprint of geopolymeric mortar: study of the contribution of the alkaline activating solution and assessment of an alternative route. RSC Adv 4:23846–23852. https://doi.org/10.1039/C4RA03375B

Miranda I, Gominho J, Mirra I, Pereira H (2012) Chemical characterization of barks from Picea abies and Pinus sylvestris after fractioning into different particle sizes. Ind Crop Prod 36:395–400. https://doi.org/10.1016/j.indcrop.2011.10.035

Mohr BJ, El-Ashkar NH, Kurtis KE (2004) Fiber-cement composites for housing construction: state-of-the-art review. In: Proc NSF hous res agenda work, p 17

Natali A, Manzi S, Bignozzi MC (2011) Novel fiber-reinforced composite materials based on sustainable geopolymer matrix. Procedia Eng 21:1124–1131. https://doi.org/10.1016/j.proeng.2011.11.2120

Neupane K, Kidd P, Chalmers D et al (2016) Investigation on compressive strength development and drying shrinkage of ambient cured powder-activated geopolymer concretes. Aust J Civ Eng 14:72–83. https://doi.org/10.1080/14488353.2016.1163765

Pacheco-Torgal F, Jalali S (2011) Cementitious building materials reinforced with vegetable fibres: a review. Constr Build Mater 25:575–581. https://doi.org/10.1016/j.conbuildmat.2010.07.024

Petermann JC, Saeed A, Hammons MI (2010) Alkali-activated geopolymers: a literature review. Air Force Res Lab. AFRL-RX-TY-TR-2010-0097. https://doi.org/10.21236/ada559113

Puertas F, Martinez-Ramirez S, Alonso S, Vazquez T (2000) Alkali-activated fly ash/slag cement: strength behavior and hydration products. Cem Concr Res 301(10):1625–1632

Sarmin SN (2016) The influence of different wood aggregates on the properties of geopolymer composites. Key Eng Mater 723:74–79. https://doi.org/10.4028/www.scientific.net/KEM.723.74

Sarmin S, Welling J (2015) Study on properties of lightweight cementitious wood composite containing fly ash/metakaolin. Pro Ligno 11:116–121

Sarmin SN, Welling J (2016) Lightweight geopolymer wood composite synthesized from alkali-activated fly ash and metakaolin. J Teknol 78:49–55. https://doi.org/10.11113/.v78.8734

Sawpan MA, Pickering KL, Fernyhough A (2011) Effect of fibre treatments on interfacial shear strength of hemp fibre reinforced polylactide and unsaturated polyester composites. Compos Part A Appl Sci Manuf 42:1189–1196. https://doi.org/10.1016/j.compositesa.2011.05.003

Sebio-Puñal T, Naya S, López-Beceiro J et al (2012) Thermogravimetric analysis of wood, holocellulose, and lignin from five wood species. J Therm Anal Calorim 109:1163–1167. https://doi.org/10.1007/s10973-011-2133-1

Shackleton R (2016) How South Africa's second most invasive tree can be managed better. In: Convers. AFRICA. http://theconversation.com/how-south-africas-second-most-invasive-tree-can-be-managed-better-62723. Accessed 13 Nov 2020

Soutsos M, Boyle AP, Vinai R et al (2016) Factors influencing the compressive strength of fly ash based geopolymers. Constr Build Mater 110(1):355–368. https://doi.org/10.1016/j.conbuildmat.2015.11.045

Tran DH, Louda P, Bortnovsky O, Bezucha P (2009) Effect of curing temperature on flexural properties of silica-based geopolymer-carbon reinforced composite. Manuf Eng 37:492–497

Valencia Saavedra WG, Mejía de Gutiérrez R (2017) Performance of geopolymer concrete composed of fly ash after exposure to elevated temperatures. Constr Build Mater 154:229–235. https://doi.org/10.1016/j.conbuildmat.2017.07.208

Van Langenberg K, Grigsby W, Ryan G (2010) Green adhesives: options for the Australian industry—summary of recent research into green adhesives from renewable materials and identification of those that are closet to commercial uptake. Forest & Wood Products Australia Project Number: PNB158-0910. Vol. 61, Issue: June, pp 10–16

Ye H, Zhang Y, Yu Z, Mu J (2018) Effects of cellulose, hemicellulose, and lignin on the morphology and mechanical properties of metakaolin-based geopolymer. Constr Build Mater 173:10–16. https://doi.org/10.1016/j.conbuildmat.2018.04.028

Yuan J, He P, Jia D et al (2016) Effect of curing temperature and SiO_2/K_2O molar ratio on the performance of metakaolin-based geopolymers. Ceram Int 42:16184–16190. https://doi.org/10.1016/j.ceramint.2016.07.139

Yunsheng Z, Wei S, Zongjin L et al (2008) Impact properties of geopolymer based extrudates incorporated with fly ash and PVA short fiber. Constr Build Mater 22:370–383. https://doi.org/10.1016/j.conbuildmat.2006.08.006

Zhang HY, Kodur V, Cao L, Qi SL (2014) Fiber reinforced geopolymers for fire resistance applications. Procedia Eng 71:153–158. https://doi.org/10.1016/j.proeng.2014.04.022